Molecular components of signal amplification in olfactory sensory cilia

Thomas Hengl, Hiroshi Kaneko[1], Kristin Dauner, Kerstin Vocke, Stephan Frings[2], and Frank Möhrlen[2]

Department of Molecular Physiology, University of Heidelberg, 69120 Heidelberg, Germany

Edited by Lily Y. Jan, University of California, San Francisco, CA, and approved January 27, 2010 (received for review August 12, 2009)

The mammalian olfactory system detects an unlimited variety of odorants with a limited set of odorant receptors. To cope with the complexity of the odor world, each odorant receptor must detect many different odorants. The demand for low odor selectivity creates problems for the transduction process: the initial transduction step, the synthesis of the second messenger cAMP, operates with low efficiency, mainly because odorants bind only briefly to their receptors. Sensory cilia of olfactory receptor neurons have developed an unusual solution to this problem. They accumulate chloride ions at rest and discharge a chloride current upon odor detection. This chloride current amplifies the receptor potential and promotes electrical excitation. We have studied this amplification process by examining identity, subcellular localization, and regulation of its molecular components. We found that the $Na^+/K^+/2Cl^-$ cotransporter NKCC1 is expressed in the ciliary membrane, where it mediates chloride accumulation into the ciliary lumen. Gene silencing experiments revealed that the activity of this transporter depends on the kinases SPAK and OSR1, which are enriched in the cilia together with their own activating kinases, WNK1 and WNK4. A second Cl^- transporter, the Cl^-/HCO_3^- exchanger SLC4A1, is expressed in the cilia and may support Cl^- accumulation. The calcium-dependent chloride channel TMEM16B (ANO2) provides a ciliary pathway for the excitatory chloride current. These findings describe a specific set of ciliary proteins involved in anion-based signal amplification. They provide a molecular concept for the unique strategy that allows olfactory sensory neurons to operate as efficient transducers of weak sensory stimuli.

chloride | olfaction | sensory transduction | transport | kinase

Mammalian olfactory receptor neurons (ORNs) present to the air a tuft of sensory cilia equipped with odorant receptors. Upon contact with odorants, these receptors actuate a transduction cascade that leads to firing of action potentials. This cascade has an unusual, two-stage organization (1). First, the activated odorant receptors induce a rise of the second messengers cAMP and Ca^{2+} in the cilia, a process that involves cAMP-gated, Ca^{2+}-permeable ion channels. In the second stage, inflowing Ca^{2+} opens Cl^- channels. By conducting a depolarizing Cl^- efflux from the cilia, these channels amplify the receptor potential approximately 10-fold, thus helping to excite the neuron even when stimulation is weak. ORNs accumulate chloride through the $Na^+/K^+/2Cl^-$ cotransporter NKCC1 and maintain an elevated intracellular Cl^- concentration (2, 3) to support amplification. Accordingly, gene ablation of NKCC1, as well as the pharmacologic suppression of Cl^- accumulation or Cl^- efflux, strongly inhibits the sensory response of ORNs (3–5). Although these observations provide a robust concept for signal amplification, several points are still unclear. These concern both the Cl^- accumulation process and the excitatory Cl^- currents. First, the site of NKCC1 expression is controversial. Although Cl^- imaging data pointed to a ciliary localization (2), immunochemical results suggested that the transporter is restricted to the dendrolateral membrane of ORNs (3). This conflict has to be solved because the site of Cl^- uptake is of prime importance for the ciliary Cl^- dynamics. Second, experiments with *Nkcc1* knockout mice have shown that NKCC1 is not the only Cl^- transporter active in ORNs (4, 5). In fact, $Nkcc1^{-/-}$ mice retain the ability to smell, a finding that points to an alternative pathway of Cl^- uptake (6). However, it is not known which additional Cl^- transporter operates in the cilia. Third, the molecular identity of the ion channels that conduct the excitatory Cl^- current is not definitely established. The best candidate protein is TMEM16B (alias ANO2) (7, 8), but it is not clear whether this protein is expressed in the sensory cilia. Here we examine these questions, and we propose a solution to each of them. Our data demonstrate that NKCC1 is highly concentrated in the ciliary layer of the olfactory epithelium. The transporter is coexpressed with the protein kinases SPAK ("STE20/SPS1-related proline/alanine-rich kinase") and OSR1 ("oxidative stress-responsive kinase-1") (9), as well as with the kinases WNK1 and WNK4 [WNK = "with no lysine (K) kinase"] (10), all of which are essential for NKCC1 activity. We find that the Cl^-/HCO_3^- exchanger SLC4A1 and the Ca^{2+}-activated Cl^- channel TMEM16B are expressed in the cilia. We propose that this set of seven chloride-related proteins represents the molecular equipment for Cl^--based signal amplification.

Results

NKCC1 Expression Is Concentrated in the Sensory Cilia. We studied the subcellular expression of NKCC1 in cryosections from rodent olfactory epithelium by immunohistochemistry, using two different antisera, C-14 and S763B. The C-14 antibody, which is directed against a C-terminal epitope of NKCC1, produced a strong immunosignal at the apical surface of rat epithelium (Fig. 1*A*). In genetically modified mice that express GFP in all mature ORNs (OMP-GFP mice) (11), we saw that the NKCC1 immunosignal originated from the top of dendritic knobs, the site of the sensory cilia (Fig. 1*B*, *Top*). In contrast, ezrin, a marker for the microvilli of supporting cells, was localized to the area between the knobs (Fig. 1*B*, *Bottom*). The NKCC1 signal in rat olfactory epithelium was also colocalized with the ciliary marker protein adenylyl cyclase III (AC III) (Fig. 1*C*, *Top*). An antiserum raised against a phosphorylated N-terminal epitope of NKCC1 (S763B) yielded a similar staining pattern (Fig. 1*C*, *Bottom*). No basolateral NKCC1 immunosignal could be distinguished from background fluorescence. These data demonstrate that the cilia are the predominant site of NKCC1 expression in the rodent olfactory epithelium.

Most of the Ciliary NKCC1 Is Phosphorylated. As the activity of NKCC1 depends on phosphorylation (12–14), we sought to estimate the degree of NKCC1 phosphorylation in olfactory cilia. The polyclonal antiserum S763B contains antibodies specific for the phosphorylated form of NKCC1 (pNKCC1) and antibodies that

Author contributions: T.H., H.K., K.D., K.V., S.F., and F.M. designed research; T.H., H.K., K.D., K.V., and F.M. performed research; T.H., H.K., K.D., K.V., S.F., and F.M. analyzed data; and S.F. wrote the paper.

The authors declare no conflict of interest.

This article is a PNAS Direct Submission.

Freely available online through the PNAS open access option.

[1]Present address: Department of Clinical Neurobiology, University Hospital of Neurology, University of Heidelberg, 69120 Heidelberg, Germany.

[2]To whom correspondence may be addressed. E-mail: s.frings@zoo.uni-heidelberg.de or moehrlen@uni-hd.de.

This article contains supporting information online at www.pnas.org/cgi/content/full/0909032107/DCSupplemental.

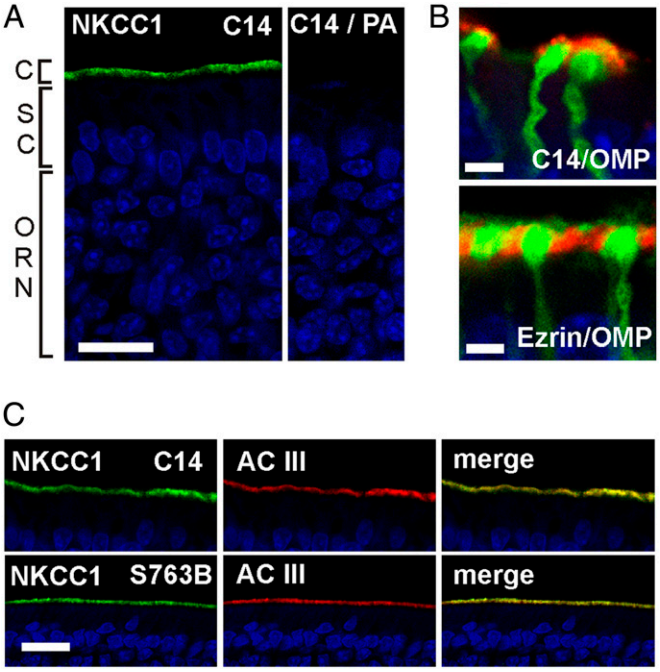

Fig. 1. Apical expression of NKCC1 in the olfactory epithelium. (*A*) Cryosections of rat olfactory epithelium stained with the NKCC1-specific antibody C14 (green) and the nuclear stain DAPI (blue). Most nuclei of the stratified epithelium belong to ORNs. The uppermost nuclear layer marks the epithelial supporting cells (SC). Dendrites of ORNs reach the apical surface of the tissue, where their cilia (C) form the chemosensory surface of the tissue. *Right:* Loss of C14 signal upon preadsorption (PA) with its antigen. (*B*) Confocal images of distal dendrites and dendritic knobs of ORNs from an OMP-GFP mouse. The NKCC1 immunosignal is on the distal surface of the knob, the microvilli-specific ezrin signal is between knobs. Only the thick proximal segments of the cilia (diameter ≈0.2 μm) are visible. The thinner distal segments (diameter <0.1 μm) are either broken off or not resolved by the confocal optics. (*C*) Staining of NKCC1 is colocalized with the ciliary marker protein AC III (red). A second NKCC1 antibody, S763B, yields a similar ciliary immunosignal (*Bottom*). Imaging parameters were adjusted so as to prevent signal saturation in the ciliary layer. Much weaker signals originating from the dendrolateral membranes could not be detected at these settings. (Scale bars, 20 μm in *A* and *C*; 2 μm in *B*.)

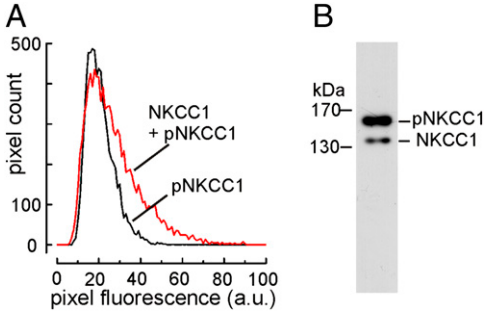

Fig. 2. Ciliary NKCC1 is highly phosphorylated. (*A*) Distribution of fluorescence intensities in the ciliary layers of consecutive cryosections stained either for phosphorylated NKCC1 (black) or for total NKCC1 (red). Each histogram illustrates the intensity distribution of ≈8.500 pixels, corresponding to ≈7,000 μm^2 of ciliary area on six cryosections. Fluorescence scaling is in arbitrary units (a.u.). (*B*) Western blot analysis of membrane proteins from olfactory epithelium stained with the NKCC1 antibody T4. The bands originating from pNKCC1 (160 kDa) and from nonphosphorylated NKCC1 (140 kDa) illustrate that the transporter exists predominantly in the phosphorylated form.

bind to nonphosphorylated NKCC1. If preadsorbed with a blocking peptide that binds those antibodies that are not phosphospecific, an immunosignal results that specifically indicates the expression of pNKCC1 (15). We prepared 18 serial cryosections from olfactory epithelium and stained consecutive sections with the S763B antiserum, alternately with and without the blocking peptide. In this way, pNKCC1 was specifically stained in every second section, whereas all NKCC1 molecules were stained in the remaining, intercalated sections. The fluorescence intensity of the resulting immunosignals was measured by image analysis. Fig. 2*A* illustrates similar distributions of ciliary fluorescence intensities for pNKCC1 and total NKCC1, indicating that a large fraction of NKCC1 is phosphorylated. To quantify this fraction, we used Western blot analysis with the monoclonal NKCC1 antibody T4, which was shown to be reliable for this method (16). The T4 antibody stained two discrete bands at 140 kDa and 160 kDa in Western blots from olfactory epithelium membrane proteins (Fig. 2*B*), which were previously identified as NKCC1 and pNKCC1 (13). Densitometric analysis of three Western blots revealed that pNKCC1 amounted to 86% ± 2.8% of the total NKCC1 content. Thus, most of the ciliary NKCC1 is phosphorylated and, therefore, presumably in a state of high transport activity.

NKCC1-Related Kinases Are Clustered in the Cilia. We next asked which protein kinases are involved in upholding this high level of phosphorylation. NKCC1 is a substrate for the two protein kinases SPAK and OSR1 (9, 12). These kinases are themselves activated by the protein kinases WNK1 and WNK4 (10), which therefore participate indirectly in the control of NKCC1 activity. In cDNA obtained from FACS-purified ORNs, NKCC1, SPAK, OSR1, WNK1, and WNK4 were present, whereas no WNK3 message was detected (Fig. 3*A*). Protein expression was examined by Western blots using antisera directed against SPAK, OSR1, WNK1, and WNK4. The antibodies labeled bands at the expected molecular size of their respective antigens (Fig. 3*B*). In cryosections of rat olfactory epithelium, the antisera directed against SPAK and OSR1 produced a robust and specific immunosignal that colocalized with AC III in the ORN cilia (Fig. 3*C*). The kinases WNK 1 and WNK 4 displayed the same polarized expression in the cilia (Fig. 3*D*). All four kinases were localized to the cilia emanating from the dendritic knobs, but they were absent from the microvilli (Fig. 3*E*). Thus, the entire complement of molecules involved in Cl^- accumulation by NKCC1 is expressed in the sensory cilia.

Phosphorylation by SPAK and OSR1 Is Necessary for NKCC1 Activity. To assess the relevance of phosphorylation for the regulation of olfactory NKCC1, we applied a functional assay that allowed us to compare NKCC1 activity at high and low levels of phosphorylation. NKCC1 activity cannot be measured directly in the cilia because the ciliary lumen is too small to permit quantitative fluorescence measurements or flux assays. We therefore turned to the *Odora* cell line, which was derived from ORN precursor cells in rat olfactory epithelium. *Odora* cells express various proteins of the olfactory signal transduction cascade and are able to respond to odorants (17, 18). RT-PCR analysis showed that they express NKCC1 together with the same set of kinases as ORNs (Fig. S1 *A* and *B*), and we developed a method to monitor NKCC1 activity using a single-cell fluorescence assay (*Materials and Methods*). This method is based on the cytosolic acidification induced by NKCC1-mediated NH_4^+ uptake (Fig. S2 *A*–*C*). The initial acidification rate r_a serves as a reliable measure for NKCC1 activity. It displays a bumetanide sensitivity with half-maximal effect of 0.03 μM bumetanide, a Cl^- dependence with an apparent K_M of 40 mM, and it depends on extracellular Na^+ (Fig. S2 *D*–*G*). Moreover, gene silencing of NKCC1 in *Odora* cells causes an 85% suppression of r_a (see below).

To reduce NKCC1 phosphorylation by SPAK and OSR1, we transfected *Odora* cells with siRNAs designed to silence the genes that encode these kinases. The mRNA levels of both kinases were reduced by >90% on the third day after siRNA transfection (Fig. S1*C*). The

NEUROSCIENCE

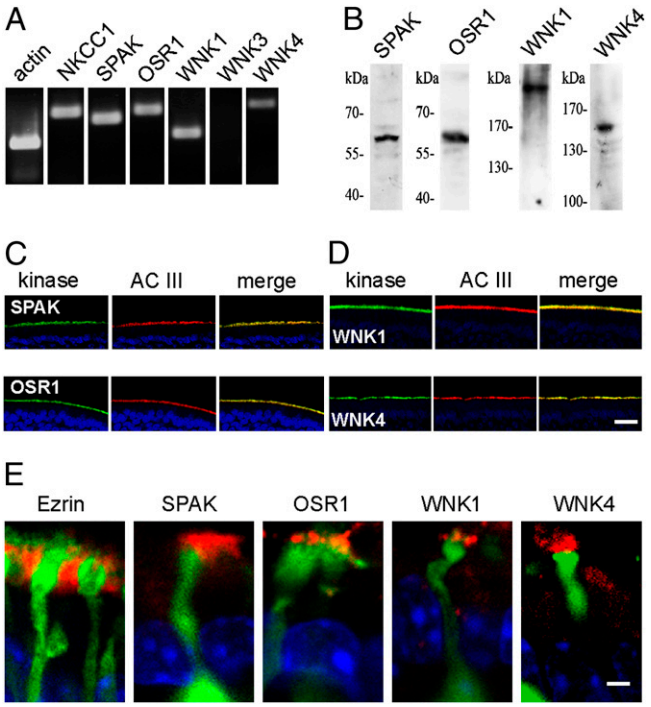

Fig. 3. Expression of NKCC1-related protein kinases in ORN cilia. (*A*) RT-PCR analysis on cDNA obtained from FACS-purified ORNs demonstrates the transcription of NKCC1 (694 bp) and of the NKCC1-related kinases SPAK (604 bp), OSR1 (734 bp), WNK1 (434 bp), and WNK4 (831 bp) in ORNs. WNK3 (753 bp) is not expressed. Actin (320 bp) served as control. (*B*) In Western blots on lysates from olfactory epithelium, kinase-specific antibodies detect the NKCC1-related kinases SPAK (60 kDa), OSR1 (58 kDa), WNK1 (250 kDa), and WNK4 (155 kDa). (*C* and *D*) Ciliary localization of NKCC1-related kinases. Immunosignals from cryosections of olfactory epithelium illustrate that the highest expression level of all four kinases is in the ciliary layer, where the kinases are colocalized with AC III. Blue signals are nuclear DAPI stains. (*E*) High-resolution images of ORN dendrites and knobs from an OMP-GFP mouse (green) illustrate that the site of kinase expression is not in the layer of supporting cell microvilli (stained by ezrin) but instead on the apical side of the dendritic knob, in the sensory cilia. [Scale bars, 20 μm in *D* (for *C* and *D*); 2 μm in *E*.]

effects of siRNA transfection on NKCC1 activity are shown in Fig. 4. Silencing either SPAK or OSR1 induced a significant reduction from the control activity. Cotransfection of both siRNAs had a similar effect, and cells transfected with both siRNAs still displayed a residual bumetanide sensitivity because 30 μM bumetanide, added 5 min before the measurement, further reduced r_a. Finally, transfecting cells with siRNA targeted at NKCC1 directly had the strongest effect. Our results demonstrated that gene silencing of NKCC1-related kinases reduced NKCC1 activity by approximately 60% (Fig. 4), providing strong qualitative evidence for the dependence of olfactory NKCC1 activity on phosphorylation.

NKCC1 Activity Is Not Controlled by Feedback Inhibition. ORNs express WNK1 and WNK4, but not WNK3 (Fig. 3*A*). This is interesting because WNK3 is thought to protect cells from excessive Cl^- accumulation, probably a vital function for neuronal inhibition in the central nervous system, the main site of WNK3 expression. Its absence from ORNs suggests that the ciliary NKCC1 transporter is not subject to feedback inhibition at elevated Cl^- concentrations and allows, instead, unrestricted Cl^- accumulation. To examine this point, we measured NKCC1 activity in *Odora* cells at various Cl^- concentrations in the cytosol. We first determined the equilibrium relation between the intracellular Cl^- concentration $[Cl^-]_i$ and the extracellular Cl^- concentration $[Cl^-]_o$. This relation was $[Cl^-]_i = 6.1\ mM + 0.7\ [Cl^-]_o$

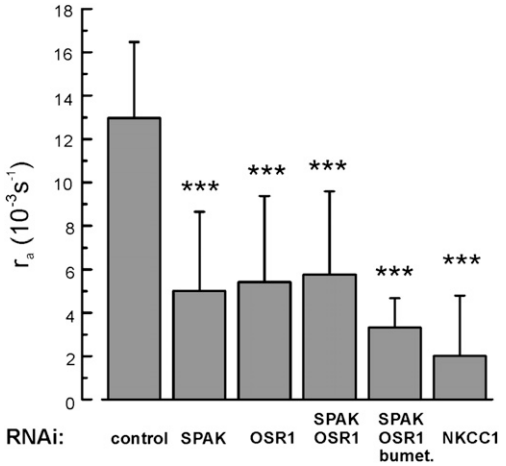

Fig. 4. Silencing of NKCC1-associated protein kinases reduces NKCC1 activity. Decrease of NKCC1 activity 3 days after siRNA transfection of *Odora* cells. Transport activity was monitored by the acidification rate r_a, which was ($13.0 \pm 3.5\ 10^{-3}s^{-1}$; 9 cells) under control conditions (cells transfected with inert siRNA) and decreased through siRNA treatment directed against SPAK ($5.0 \pm 3.6\ 10^{-3}s^{-1}$; 7 cells), OSR1 ($5.4 \pm 3.9\ 10^{-3}s^{-1}$; 9 cells), and both SPAK and OSR1 ($5.7 \pm 3.8\ 10^{-3}s^{-1}$; 10 cells). This treatment left a residual NKCC1 activity that could be inhibited by 30 μM bumetanide ($3.3 \pm 1.4\ 10^{-3}s^{-1}$; 3 cells). Gene silencing of NKCC1 itself reduced the activity to a similar level ($2.0 \pm 2.8\ 10^{-3}s^{-1}$; 5 cells). Thus, gene silencing of the NKCC1-associated kinases reduced NKCC1 activity by ≈60%.

(Fig. S3). To measure the initial acidification rate at a test value of $[Cl^-]_i$, cells were first held at the corresponding $[Cl^-]_o$ for 30 min to allow equilibration according to this relation. The extracellular solution was then stepped to 150 mM $[Cl^-]_o$ plus 5 mM NH_4^+, and r_a was measured. Fig. 5*A* shows that r_a declined with increasing values of $[Cl^-]_i$. The data were fitted with $r_a = r_a^{max} - (r_a^{max} \times [Cl^-]_i)/([Cl^-]_i) + K_M)$, with $r_a^{max} = 30 \times 10^{-3}s^{-1}$ and $K_M = 30$ mM. Plotting these r_a values against the free energy for NKCC1-mediated transport:

$$\Delta G = RT \cdot \ln \frac{[Na]_i [K]_i [Cl]_i^2}{[Na]_o [K]_o [Cl]_o^2}$$

showed that the dependence of r_a on ΔG was logarithmic (Fig. 5*B*). This indicates that the Na^+/K^+-coupled Cl^- uptake into

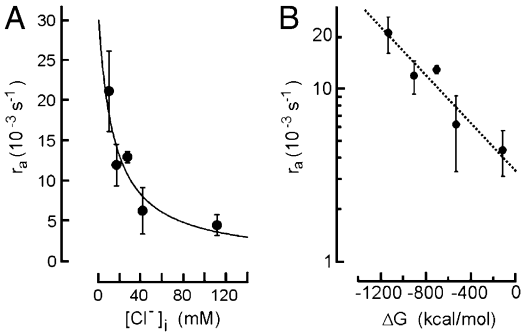

Fig. 5. NKCC1 activity at high levels of intracellular Cl^-. (*A*) Transport activity monitored by the initial acidification rate r_a at $[Cl^-]_o$ = 150 mM and increasing intracellular Cl^- concentrations $[Cl^-]_i$. (*B*) Relation between r_a and the calculated driving force for NKCC1. Data from *A* do not deviate from the simple logarithmic relation that characterizes the dependence of NKCC1 transport rate on the free energy, ΔG, of the coupled transport. No evidence is detectable for transport inhibition at high levels of $[Cl^-]_i$.

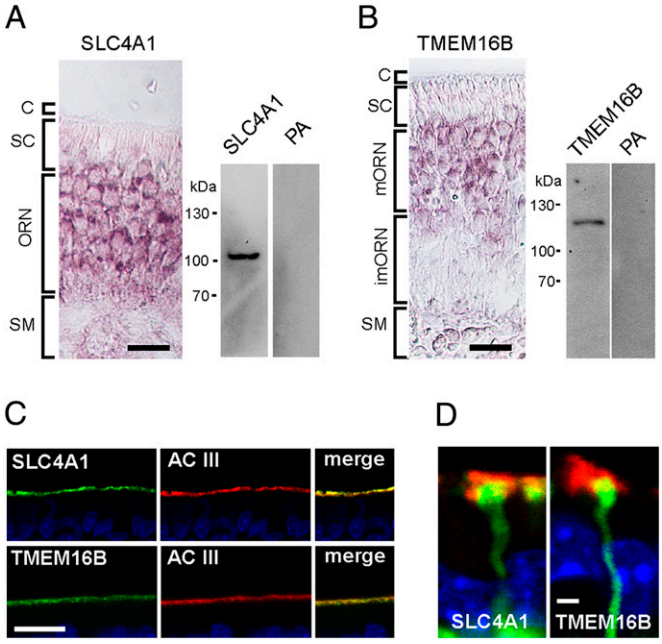

Fig. 6. Expression of SLC4A1 and TMEM16B in sensory cilia. (*A*) In situ hybridization of an SLC4A1 antisense RNA probe illustrates the transcription of the exchanger gene in ORNs but not in supporting cells (SC) and submucosal tissue (SM). (*Right*) Western blot analysis with an SLC4A1-specific antiserum detects a single band at 100 kDa in protein extract from olfactory epithelium. The signal is abolished by preadsorption to the antigen (PA). (*B*) In situ hybridization of a TMEM16B antisense RNA probe illustrates the transcription of the channel gene in mature ORNs (mORN) but not in immature neurons (imORNs), supporting cells (SC), or submucosal tissue (SM). (*Right*) Western blot analysis with a TMEM16B-specific antiserum detects a single band at 110 kDa in protein extracts from olfactory epithelium. The signal is abolished by preadsorption to the antigen (PA). (*C*) The antisera against SLC4A1 and TMEM16B specifically stain cilia in cryosections from olfactory epithelium, where the proteins colocalize with AC III. Blue signals are nuclear DAPI stains. (*D*) High-resolution images of single dendritic knobs from an OMP-GFP mouse illustrate that the expression of SLC4A1 and TMEM16B is detected in the proximal cilia. (Scale bars, 20 μm in *A*–*C*; 2 μm in *D*).

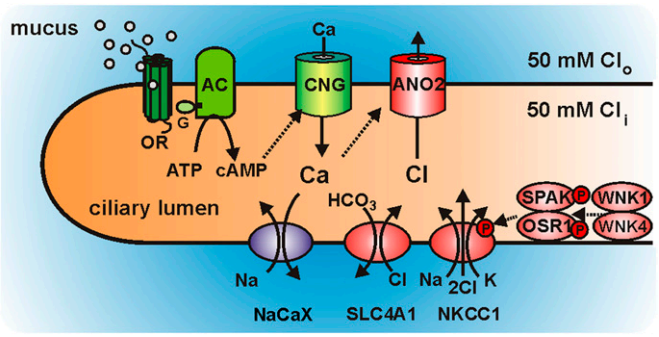

Fig. 7. Signal amplification strategy of olfactory sensory cilia. Model depicting the interplay of transduction proteins (green) and amplification proteins (red) in a sensory cilium as outlined in the text. AC, adenylyl cyclase III; ANO2, Ca^{2+}-activated Cl^- channels containing the protein TMEM16B/ANO2; CNG, cAMP-gated cation channel; G, GTP-binding protein G_{olf}; NaCaX, Na^+/Ca^{2+} exchanger; NKCC1, $Na^+/K^+/2Cl^-$ cotransporter; OR, olfactory receptor; OSR1, oxidative stress-responsive kinase-1; SLC4A1, Cl^-/HCO_3^- exchanger; SPAK, STE20/SPS1-related proline/alanine-rich kinase; WNK1 and WNK4, with no lysine (K) kinases.

Odora cells is solely governed by the driving forces of the contributing ions. It does not point to any Cl^--dependent inhibition. In case of an inhibitory feedback the plot in Fig. 5*B* would deviate from linearity at elevated $[Cl^-]_i$ levels (19). Our results demonstrate the lack of feedback inhibition on NKCC1 at elevated levels of $[Cl^-]_i$, a finding that is consistent with the lack of WNK3 expression in ORNs.

Sensory Cilia Express the Cl^-/HCO_3^- Exchanger SLC4A1. In the ciliary proteome, the most prominent Cl^- transporter apart from NKCC1 is SLC4A1 (20). We found mRNA encoding this transporter in cDNA from FACS-purified ORNs, and we localized its mRNA specifically to ORNs using in situ hybridization (Fig. 6*A*). SLC4A1 message was not detected in supporting cells, nor was it expressed in respiratory epithelium. Using a SLC4A1-specific antiserum, we observed a single band at the appropriate molecular size of 100 kDa in Western blots prepared from olfactory epithelial proteins (Fig. 6*A*). In cryosections the antiserum revealed virtually exclusive expression at the apical surface of the olfactory epithelium, where SLC4A1 was coexpressed with AC III (Fig. 6*C*, *Top*). Expression was localized to the proximal segments of the cilia (Fig. 6*D*).

Sensory Cilia Express the Ca^{2+}-Activated Cl^- Channel TMEM16B (ANO2). The ciliary proteome contains one prominent Ca^{2+}-activated Cl^- channel: TMEM16B (alias: ANO2). The family of TMEM16 (alias: anoctamin) proteins have recently been shown to form Ca^{2+}-activated Cl^- channels (7, 21–24). The mRNA of this protein was located in rodent ORNs (8, 25), and TMEM16B is the only of the 10 TMEM16 isoforms present in the ciliary proteome (8, 20). We detected the mRNA expression of TMEM16B in cDNA obtained from ORNs that were FACS purified. In situ hybridization revealed that the message was specifically expressed in mature ORNs (Fig. 6*B*). The message was absent from immature ORNs as well as from supporting cells and from the respiratory epithelium. We generated an isoform-specific polyclonal antiserum that was affinity purified and used for Western blot analyses. It stained a single band at 110 kDa, the predicted molecular size of TMEM16B (Fig. 6*B*, *Right*). In cryosections from rat olfactory epithelium, the antiserum produced an immunosignal specifically in the cilia, where it colocalized with AC III (Fig. 6*C*, *Bottom*). Higher resolution shows expression of the channel in the proximal cilia (Fig. 6*D*).

Discussion

Each odorant receptor in the mammalian nose has a wide spectrum of cognate ligands. This enables the olfactory system to detect and distinguish a practically unlimited variety of chemical substances with only approximately 1,000 different odorant receptors (26–28). In fact, odor discrimination is a combinatorial process; the sensory information is not contained in the response of a single ORN but in the combined activity of all ORNs. Although the read-out from many low-selectivity receptors can provide precise sensory information (29), the weak interaction between odorants and their receptors constitutes a severe problem for signal transduction. Bhandawat et al. (30) have demonstrated that the dwell time of an odorant at its receptor is less than 1 ms. This brief interval limits the activation of the GTP-binding protein G_{olf} and its target enzyme AC III in the ciliary membrane. Indeed, the rate of odor-induced cAMP synthesis in the ciliary lumen was shown to be in the range of 10–50 μM/s in amphibian ORNs (31). Odor discrimination happens within 100 ms after contact with the stimulus (32, 33), and the cAMP concentrations can reach only a few micromolars within this time. Although the physiologic cAMP levels during normal sniffing have not been measured in mammals yet, it is clear that ORNs have to operate at very low second-messenger concentrations. The solution seems to be the chloride-based signal amplification, for which the ORN cilia are perfectly equipped.

Cl^- Accumulation from the Mucosal Fluid: NKCC1 and SLC4A1. In the rodent olfactory epithelium, we find NKCC1 expression only in ORNs. This observation is in accordance with the earlier result that

NEUROSCIENCE

Nkcc1 promotor activity in this tissue is restricted to ORNs and is absent from supporting cells (3). In an electron microscopic study in rat olfactory epithelium, the T4 antibody reported NKCC1 expression in supporting cells as well as in ORN cilia (34). Because the *Nkcc1* gene is not expressed in supporting cells (3), and because the T4 antibody shows nonspecific staining in retina (35), these data must be interpreted as a cross-reaction of T4. The transport activity of NKCC1 depends on the phosphorylation of four threonine residues in its N terminus (Thr-194, Thr-198, Thr-203, and Thr-208 in rat NKCC1). The kinases that mediate NKCC1 phosphorylation are SPAK and OSR1, both members of the germinal center kinase (GCK)-VI subfamily (9, 12, 36–38). Both kinases are regulated by the WNK family of protein kinases (10). Through their effects on SPAK/OSR1, WNK kinases control members of the SLC12 family of Cl^-/cation cotransporters (NKCCs, KCCs, NCC) and thereby play a pivotal role in cellular Cl^- homeostasis (39). Recent studies have revealed that WNK1 and WNK4 phosphorylate OSR1 and SPAK (40–43) and thereby promote phosphorylation and activation of NKCC1. Our data show that all four kinases, SPAK, OSR1, WNK1, and WNK4, are expressed in ORN cilia, and SPAK and OSR1 are both necessary for maximal activation of the transporter. The five proteins are thought to form a supramolecular complex: SPAK and OSR1 bind to NKCC1 (44), whereas WNK1 and WNK4 bind to SPAK/OSR1 (42, 43). The kinase WNK3 is absent from ORNs. Among the four WNK kinases, WNK3 shows the highest expression in the brain, and WNK3 is thought to act as a Cl^- sensor involved in protecting cells from excessive Cl^- accumulation (45–47). The absence of WNK3 from ORNs, the simple thermodynamic basis of NKCC1 activity seen in our transport assay, and the absence of the main neuronal Cl^- exporter KCC2 (2) all illustrate that these neurons dispense with means for intracellular Cl^- reduction and instead optimize Cl^- accumulation.

Olfactory cilia are embedded in the mucosal fluid, a medium with a distinct ion composition including ≈50 mM Cl^- (48). In a study of Cl^- dynamics in the olfactory epithelium (2) we observed a standing intracellular Cl^- gradient in ORNs when extracellular Cl^- was stepped from 50 mM to 150 mM. The orientation of this gradient indicated that Cl^- entered the ORNs via the cilia. In contrast to this notion, immunohistochemical examinations of *Nkcc1*$^{+/-}$ mice suggested that the transporter was only expressed in the dendrosomatic membrane of ORNs (3), whereas our data clearly show a polarized, ciliary expression. This discrepancy may reflect differences in tissue treatment or problems with antigen recognition by the antibodies used, but the precise reason for these inconsistent results is not known. We would like to stress that our data demonstrated consistently the ciliary colocalization of five different proteins, which all must coassemble for effective Cl^- accumulation. Together with the prominent representation of NKCC1 in the ciliary proteome (8, 20) and the functional evidence for Cl^- uptake through the cilia (2), this polarized expression of the entire Cl^- accumulation complex represents compelling evidence for the hypothesis that ORN cilia obtain their Cl^- primarily from the mucosal fluid.

ORNs of *Nkcc1*$^{-/-}$ mice retain substantial Cl^- accumulation (4, 5). This Cl^- uptake pathway is sensitive to DIDS (4,4′-diisothiocyanatostilbene-2,2′-disulfonic acid) and contributes approximately 40% to the total Cl^- accumulation capacity. Our data obtained by proteomics and immunochemistry demonstrate that the Cl^-/HCO_3^- exchanger SLC4A1 is expressed in the ORN cilia. This finding points to an additional route for ciliary Cl^- uptake, one that does not depend on cation cotransport. It seems that the cilia are able to fuel Cl^- uptake by synthesizing HCO_3^- from CO_2, thus driving ciliary SLC4A1 to accumulate Cl^-. The precise contribution of this transport pathway needs to be examined under in vivo conditions with respect to pH buffering, CO_2 concentration, and Cl^- activity. Taken together, our data indicate that the cilia of ORNs accumulate Cl^- predominantly from the mucosal fluid.

Excitatory Cl^- Current. The *TMEM16B* gene is selectively transcribed in mature ORNs, and protein expression is limited to the sensory cilia. This finding is consistent with electrophysiologic measurements from native Ca^{2+}-activated Cl^- channels (49, 50). Two recent reports on the heterologous expression of TMEM16B in HEK 293 cells (7, 8) revealed that TMEM16B produced Ca^{2+}-activated Cl^- channels with functional properties that closely matched the properties of native Ca^{2+}-activated Cl^- channels examined in the ciliary membrane by patch-clamp analysis (51). Moreover, when a TMEM16B-EGFP fusion protein was expressed in olfactory epithelium by adenoviral gene transfer, the protein was detected in somata, dendrites, and cilia (8), demonstrating that TMEM16B is able to use the ciliary targeting machinery. Together, these findings strongly support the hypothesis that TMEM16B is part of the ciliary Cl^- channel and may contribute to the excitatory Cl^- current during odor detection.

Molecular Concept: Increasing the Gain of Olfactory Transduction. Because of the weak interaction of odorants with their receptors, the initial metabotropic transduction step (Fig. 7, green), the odor-induced synthesis of cAMP, operates with low efficiency (30, 31). A few μM cAMP is, however, sufficient to activate the cAMP-gated transduction channels. These channels respond to 1–10 μM cAMP, conduct Ca^{2+} and monovalent cations into the ciliary lumen (52, 53), and generate an initial receptor potential that amounts to <10% of the total receptor potential, as can be gleaned from electroolfactographic measurements in mice. The cAMP-dependent Ca^{2+} influx serves as a trigger that sets off a much larger Cl^- efflux. To maintain these Cl^- currents, the cilia express an entire complement of proteins involved in Cl^- accumulation (Fig. 7, red), with NKCC1 and SLC4A1 providing the pathways for Cl^- uptake. Chloride accumulation operates continuously and maintains the ciliary Cl^- concentration at the level of the mucosal fluid (≈50 mM). These processes charge the resting cilium with Cl^- and enable it to discharge a large, excitatory Cl^- efflux through TMEM16B-containing channels in response to odor stimulation. The output of the cilium is an electrical signal that elicits action potentials in the dendritic membrane (54).

Materials and Methods

Animals. Olfactory epithelium was obtained from 6–24-week-old Wistar rats and OMP-GFP mice. All experimental procedures were performed in accordance with the Animal Protection Law and the guidelines and permissions of Heidelberg University.

Molecular Characterization of Transcripts and Proteins. For technical details on FACS purification of ORNs, on RT-PCR, in situ hybridization, generation of antisera, immunohistochemistry, Western blots, and gene silencing, see *SI Materials and Methods*.

NKCC1 Activity Assay. *Odora* cells (17) were kindly provided by Dr. Dale Hunter (Tufts University) and cultivated in minimum essential medium (M2279; Sigma-Aldrich), supplemented with 10% FBS (F7524; Sigma-Aldrich), 1% penicillin/streptomycin (G6784; Sigma-Aldrich), and 1% nonessential amino acids (M7145; Sigma-Aldrich) at 33 °C, 7% CO_2. Cells were incubated with 17.6 μM SNARF-1(Molecular Probes, Invitrogen) for 1 h at room temperature. The bath solution contained (in mM) 140 NaCl, 5 KCl, 2 $CaCl_2$, 1 $MgCl_2$, 10 glucose, and 10 Hepes, pH 7.4 (NaOH). For the assay, a single cell was excited at 510 nm, and fluorescence emission was recorded (λ_{em} = 580 and 640 nm) through a 40×/n.a. 1.2 oil immersion lens by two photomultipliers. The fluorescence intensity signals were low-pass filtered at 30 Hz, sampled at 100 Hz, and stored with a self-written program. To determine NKCC1 activity, we measured the bumetanide-sensitive fraction of the pH change induced by NH_4^+ uptake during the application of 5 mM NH_4Cl (replacing KCl). The initial phase of acidification was analyzed for NKCC1 activity according to $dpH/dt = -\Delta pH/\tau = r_a$. The two parameters ΔpH and τ were obtained by fitting the relation $[pH(t) = pH^0 + \Delta pH \times \exp(-t/\tau)]$ to the time course of acidification, as described in Fig. S2.

ACKNOWLEDGMENTS. We thank Dr. Dale Hunter (Tufts University) for supplying the *Odora* cells; Dr. Biff Forbush (Yale University) for help with NKCC1 antisera; and Jessica Maier, Inka Schäfer, and Michaela Schmidt for contributions to this project. This work was supported by the Deutsche Forschungsgemeinschaft (Fr 937/10 and MO1384/2).

1. Kleene SJ (2008) The electrochemical basis of odor transduction in vertebrate olfactory cilia. *Chem Senses* 33:839–859.
2. Kaneko H, Putzier I, Frings S, Kaupp UB, Gensch T (2004) Chloride accumulation in mammalian olfactory sensory neurons. *J Neurosci* 24:7931–7938.
3. Reisert J, Lai J, Yau KW, Bradley J (2005) Mechanism of the excitatory Cl^- response in mouse olfactory receptor neurons. *Neuron* 45:553–561.
4. Nickell WT, Kleene NK, Gesteland RC, Kleene SJ (2006) Neuronal chloride accumulation in olfactory epithelium of mice lacking NKCC1. *J Neurophysiol* 95:2003–2006.
5. Nickell WT, Kleene NK, Kleene SJ (2007) Mechanisms of neuronal chloride accumulation in intact mouse olfactory epithelium. *J Physiol* 583:1005–1020.
6. Smith DW, Thach S, Marshall EL, Mendoza MG, Kleene SJ (2008) Mice lacking NKCC1 have normal olfactory sensitivity. *Physiol Behav* 93:44–49.
7. Pifferi S, Dibattista M, Menini A (2009) TMEM16B induces chloride currents activated by calcium in mammalian cells. *Pflugers Arch* 458:1023–1038.
8. Stephan AB, et al. (2009) ANO2 is the cilial calcium-activated chloride channel that may mediate olfactory amplification. *Proc Natl Acad Sci USA* 106:11776–11781.
9. Delpire E, Gagnon KB (2008) SPAK and OSR1: STE20 kinases involved in the regulation of ion homoeostasis and volume control in mammalian cells. *Biochem J* 409:321–331.
10. Kahle KT, Ring AM, Lifton RP (2008) Molecular physiology of the WNK kinases. *Annu Rev Physiol* 70:329–355.
11. Potter SM, et al. (2001) Structure and emergence of specific olfactory glomeruli in the mouse. *J Neurosci* 21:9713–9723.
12. Giménez I (2006) Molecular mechanisms and regulation of furosemide-sensitive Na-K-Cl cotransporters. *Curr Opin Nephrol Hypertens* 15:517–523.
13. Flemmer AW, Gimenez I, Dowd BF, Darman RB, Forbush B (2002) Activation of the Na-K-Cl cotransporter NKCC1 detected with a phospho-specific antibody. *J Biol Chem* 277:37551–37558.
14. Darman RB, Forbush B (2002) A regulatory locus of phosphorylation in the N terminus of the Na-K-Cl cotransporter, NKCC1. *J Biol Chem* 277:37542–37550.
15. Funk K, et al. (2008) Modulation of chloride homeostasis by inflammatory mediators in dorsal root ganglion neurons. *Mol Pain* 4:32.
16. Lytle C, Xu JC, Biemesderfer D, Forbush B, 3rd (1995) Distribution and diversity of Na-K-Cl cotransport proteins: A study with monoclonal antibodies. *Am J Physiol* 269: C1496–C1505.
17. Murrell JR, Hunter DD (1999) An olfactory sensory neuron line, odora, properly targets olfactory proteins and responds to odorants. *J Neurosci* 19:8260–8270.
18. Kaneko H, Möhrlen F, Frings S (2006) Calmodulin contributes to gating control in olfactory calcium-activated chloride channels. *J Gen Physiol* 127:737–748.
19. Rocha-González HI, Mao S, Alvarez-Leefmans FJ (2008) Na+,K+,2Cl- cotransport and intracellular chloride regulation in rat primary sensory neurons: Thermodynamic and kinetic aspects. *J Neurophysiol* 100:169–184.
20. Mayer U, et al. (2009) The proteome of rat olfactory sensory cilia. *Proteomics* 9: 322–334.
21. Schroeder BC, Cheng T, Jan YN, Jan LY (2008) Expression cloning of TMEM16A as a calcium-activated chloride channel subunit. *Cell* 134:1019–1029.
22. Yang YD, et al. (2008) TMEM16A confers receptor-activated calcium-dependent chloride conductance. *Nature* 455:1210–1215.
23. Caputo A, et al. (2008) TMEM16A, a membrane protein associated with calcium-dependent chloride channel activity. *Science* 322:590–594.
24. Hartzell HC, Yu K, Xiao Q, Chien LT, Qu Z (2009) Anoctamin/TMEM16 family members are Ca2+-activated Cl- channels. *J Physiol* 587:2127–2139.
25. Yu TT, et al. (2005) Differentially expressed transcripts from phenotypically identified olfactory sensory neurons. *J Comp Neurol* 483:251–262.
26. Buck L, Axel R (1991) A novel multigene family may encode odorant receptors: A molecular basis for odor recognition. *Cell* 65:175–187.
27. Keller A, Vosshall LB (2008) Better smelling through genetics: Mammalian odor perception. *Curr Opin Neurobiol* 18:364–369.
28. Reisert J, Restrepo D (2009) Molecular tuning of odorant receptors and its implication for odor signal processing. *Chem Senses* 34:535–545.
29. Wilson RI, Mainen ZF (2006) Early events in olfactory processing. *Annu Rev Neurosci* 29:163–201.
30. Bhandawat V, Reisert J, Yau KW (2005) Elementary response of olfactory receptor neurons to odorants. *Science* 308:1931–1934.
31. Takeuchi H, Kurahashi T (2005) Mechanism of signal amplification in the olfactory sensory cilia. *J Neurosci* 25:11084–11091.
32. Wesson DW, Carey RM, Verhagen JV, Wachowiak M (2008) Rapid encoding and perception of novel odors in the rat. *PLoS Biol* 6:e82.
33. Carey RM, Verhagen JV, Wesson DW, Pírez N, Wachowiak M (2009) Temporal structure of receptor neuron input to the olfactory bulb imaged in behaving rats. *J Neurophysiol* 101:1073–1088.
34. Menco BP (2005) The fine-structural distribution of G-protein receptor kinase 3, beta-arrestin-2, Ca2+/calmodulin-dependent protein kinase II and phosphodiesterase PDE1C2, and a Cl(-)-cotransporter in rodent olfactory epithelia. *J Neurocytol* 34:11–36.
35. Zhang LL, Delpire E, Vardi N (2007) NKCC1 does not accumulate chloride in developing retinal neurons. *J Neurophysiol* 98:266–277.
36. Dowd BF, Forbush B (2003) PASK (proline-alanine-rich STE20-related kinase), a regulatory kinase of the Na-K-Cl cotransporter (NKCC1). *J Biol Chem* 278: 27347–27353.
37. Geng Y, Hoke A, Delpire E (2009) The Ste20 kinases Ste20-related proline-alanine-rich kinase and oxidative-stress response 1 regulate NKCC1 function in sensory neurons. *J Biol Chem* 284:14020–14028.
38. Delpire E (2009) The mammalian family of sterile 20p-like protein kinases. *Pflugers Arch* 458:953–967.
39. Kahle KT, et al. (2006) WNK protein kinases modulate cellular Cl- flux by altering the phosphorylation state of the Na-K-Cl and K-Cl cotransporters. *Physiology (Bethesda)* 21:326–335.
40. Gagnon KB, England R, Delpire E (2006) Volume sensitivity of cation-Cl- cotransporters is modulated by the interaction of two kinases: Ste20-related proline-alanine-rich kinase and WNK4. *Am J Physiol Cell Physiol* 290:C134–C142.
41. Vitari AC, et al. (2006) Functional interactions of the SPAK/OSR1 kinases with their upstream activator WNK1 and downstream substrate NKCC1. *Biochem J* 397:223–231.
42. Vitari AC, Deak M, Morrice NA, Alessi DR (2005) The WNK1 and WNK4 protein kinases that are mutated in Gordon's hypertension syndrome phosphorylate and activate SPAK and OSR1 protein kinases. *Biochem J* 391:17–24.
43. Anselmo AN, et al. (2006) WNK1 and OSR1 regulate the Na+, K+, 2Cl- cotransporter in HeLa cells. *Proc Natl Acad Sci USA* 103:10883–10888.
44. Gagnon KB, England R, Delpire E (2007) A single binding motif is required for SPAK activation of the Na-K-2Cl cotransporter. *Cell Physiol Biochem* 20:131–142.
45. Kahle KT, et al. (2005) WNK3 modulates transport of Cl- in and out of cells: Implications for control of cell volume and neuronal excitability. *Proc Natl Acad Sci USA* 102:16783–16788.
46. de Los Heros P, et al. (2006) WNK3 bypasses the tonicity requirement for K-Cl cotransporter activation via a phosphatase-dependent pathway. *Proc Natl Acad Sci USA* 103:1976–1981.
47. Ponce-Coria J, et al. (2008) Regulation of NKCC2 by a chloride-sensing mechanism involving the WNK3 and SPAK kinases. *Proc Natl Acad Sci USA* 105:8458–8463.
48. Reuter D, Zierold K, Schröder WH, Frings S (1998) A depolarizing chloride current contributes to chemoelectrical transduction in olfactory sensory neurons in situ. *J Neurosci* 18:6623–6630.
49. Kleene SJ (1993) Origin of the chloride current in olfactory transduction. *Neuron* 11: 123–132.
50. Eberius C, Schild D (2001) Local photolysis using tapered quartz fibres. *Pflugers Arch* 443:323–330.
51. Reisert J, Bauer PJ, Yau KW, Frings S (2003) The Ca-activated Cl channel and its control in rat olfactory receptor neurons. *J Gen Physiol* 122:349–363.
52. Leinders-Zufall T, Rand MN, Shepherd GM, Greer CA, Zufall F (1997) Calcium entry through cyclic nucleotide-gated channels in individual cilia of olfactory receptor cells: Spatiotemporal dynamics. *J Neurosci* 17:4136–4148.
53. Dzeja C, Hagen V, Kaupp UB, Frings S (1999) Ca2+ permeation in cyclic nucleotide-gated channels. *EMBO J* 18:131–144.
54. Dubin AE, Dionne VE (1994) Action potentials and chemosensitive conductances in the dendrites of olfactory neurons suggest new features for odor transduction. *J Gen Physiol* 103:181–201.